Electronic Supplementary Material (ESI) for Analyst.

Supporting Information

Ratiometric electrochemical sensing based on Mo_2C for detection of acetaminophen

Tingting Zhu[a, 1], Hailong Ren[a,1], Wencui Liang[a], Yangguang Li[a], Yuwen Xu[a], Miaojuan Dai[a], Bang-Ce Ye[a,b,*]

[a] Key Laboratory for Green Processing of Chemical Engineering of Xinjiang Bingtuan, School of Chemistry and Chemical Engineering, Shihezi University, Shihezi 832003, China
[b] Lab of Biosystem and Microanalysis, Institute of Engineering Biology and Health, State Key Laboratory of Bioreactor Engineering, East China University of Science and Technology, Shanghai 200237, China

[1] These authors contributed equally to this work.

* Corresponding authors. Tel/Fax: +86-021-64252094. E-mail address: bcye@ecust.edu.cn

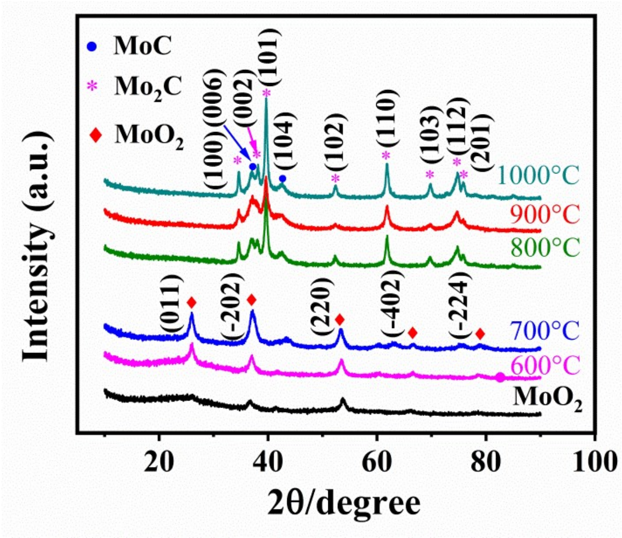

Fig. S1 XRD patterns of MoO_2 and Mo_2C

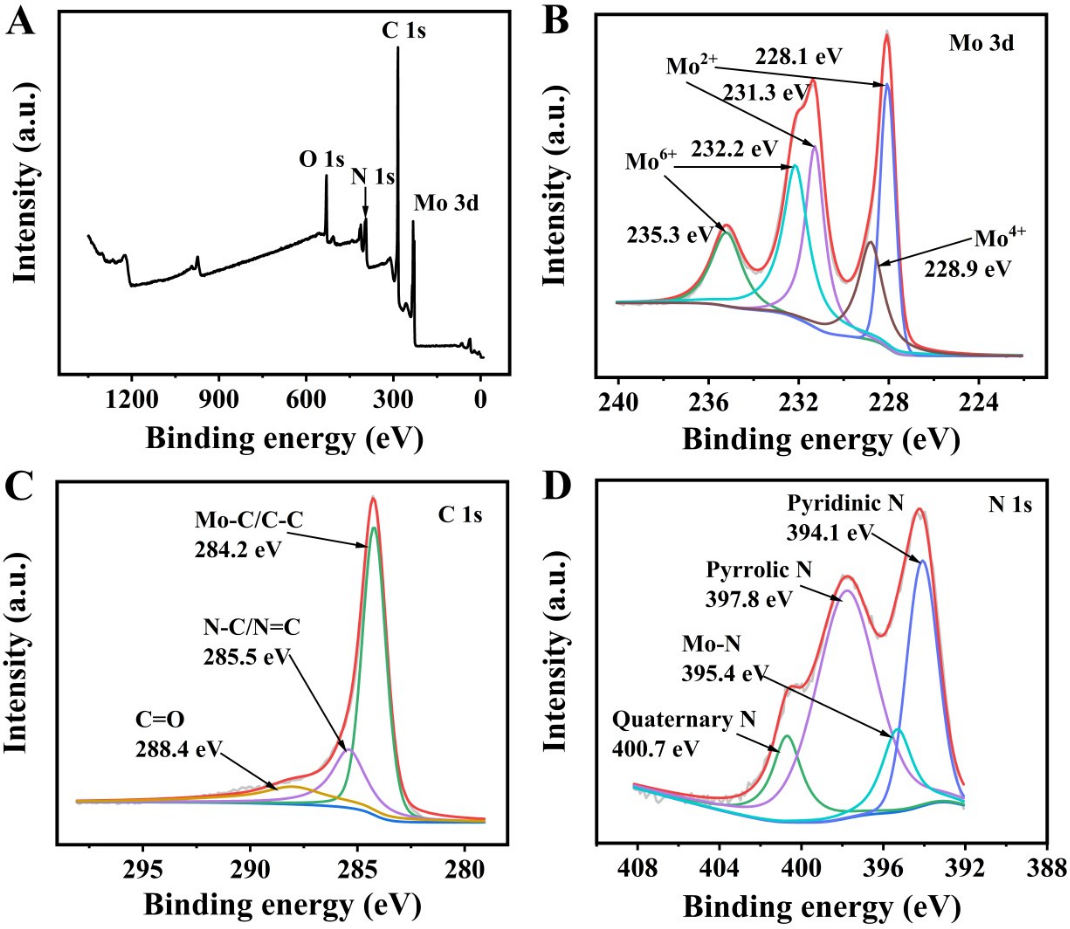

Fig. S2 XPS survey spectrum of N-Mo_2C (A) and the high-resolution XPS spectra of (B) Mo 3d, (C) C 1s and (D) N 1s.

1 Optimization of experimental conditions

1.1 Annealing temperature optimization of Mo_2C

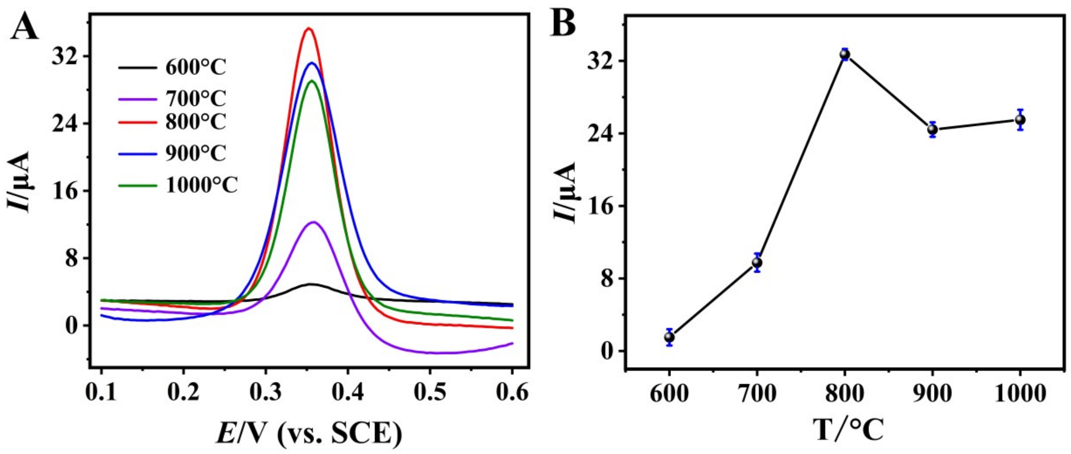

Fig. S3 (A) SWV of Mo_2C modified GCE in 10 µM AP at different temperatures, (B) Relationship between different annealing temperatures and AP peak current

The effect of annealing temperature of Mo_2C on the electrocatalytic properties of 10 µm AP was optimized. As shown in Fig. S3, as the annealing temperature increases from 500°C to 900°C, the oxidation peak current of AP increases, and the maximum peak current is obtained at 800°C. Further increase of annealing temperature results in a decrease of peak current of AP. From Fig. S4, it can be seen that the specific surface area of MoO_2 is the smallest before carbonization. As the temperature increases from 600°C to 800°C, the specific surface area reaches the maximum at 800 °C, and the specific surface area gradually decreasing over 800 °C may be because the carbonization temperature is too high causing the organic ligand volatilizing, resulting in a decrease in the specific surface area of the framework collapse. Therefore, the carbonization temperature of 800°C was selected as the optimal condition for Mo_2C synthesis.

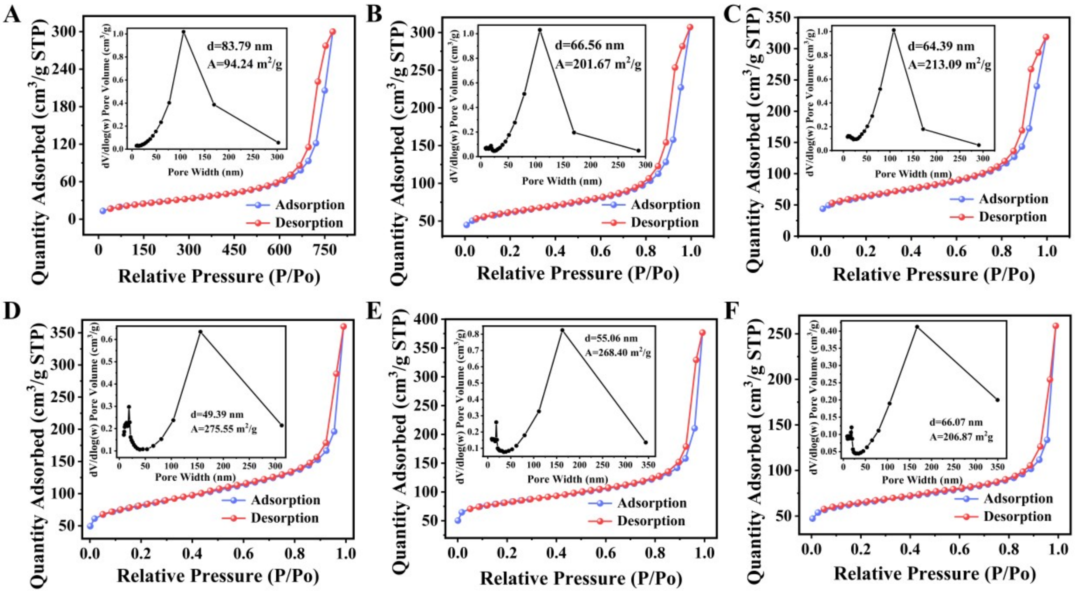

Fig. S4 (A) N_2 adsorption-desorption curves of MoO_2 (A) and Mo_2C at different annealing temperatures （B）600°C（C）700°C（D）800°C（E）900°C（F）1000°C. (Insets are the corresponding pore size distribution)

1.2 Optimizing volume of Mo_2C

The relationship between Mo_2C drop coating amount and AP peak current is shown in Fig. S5. When the amount of Mo_2C is 3 μL, the oxidation peak current of AP reaches the maximum value. In order to improve the sensitivity of the electrode, 3 μL was selected as the optimal amount of Mo_2C.

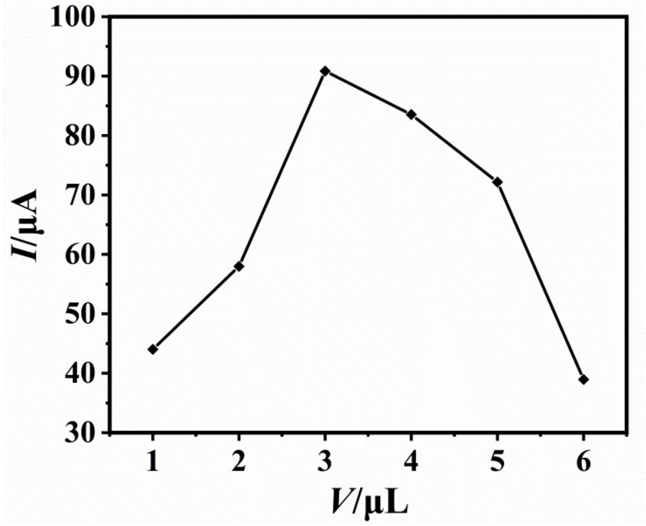

Fig. S5 The relation between AP of redox peak current and volume of Mo_2C

1.3 Influence of scan rate

In order to determine the electrochemical mechanism of AP on Mo_2C/GCE, the relationship between the redox peak current and scan rate was investigated by cyclic voltammetry (CV). It can be seen from Fig. S6A that when the scan rate increases from 10 mV s^{-1} to 200 mV s^{-1}, the redox peak current of AP increases, which indicates that the electrochemical reaction of AP on Mo_2C/GCE is an adsorption control process. The redox peak current of AP has a linear relationship with the scan rate (Fig. S6B), indicating that the electrochemical reaction of AP in Mo_2C/GCE is a surface control process [1].

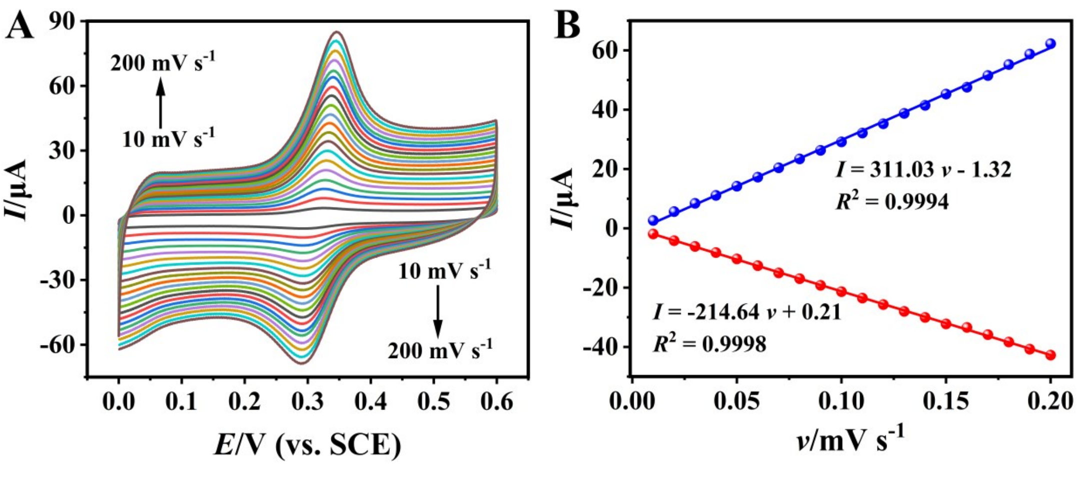

Fig. S6 (A) CV curves of 10 μM AP at Mo_2C/GCE in 0.1 M PBS (pH 6.0) with different scan rates (10~200 mV s^{-1}). The relationship between redox peak currents and the square root of the scan rate for (B) AP. The blue line represents the oxidation peak and the red line refers to the reduction peak.

1.4 Influence of pH

The pH value of the solution can affect the redox peak current value of the analyte, so that the redox peak potential can be shifted positively or negatively to affect the electrochemical reaction. Therefore, it is necessary to maximize the redox peak current at a low peak potential under the optimal pH conditions. The electrochemical behavior of 10 μM AP with different pH in Mo_2C/GCE was investigated by SWV (Fig. S7A). As shown in Fig. S7B, as the pH value increases from 4.0 to 9.0, the peak current first increases and then decreases, and the response is the greatest when the pH value is 6.0. In order to further understand the mechanism of electrocatalytic oxidation of AP, the relationship between peak potential and pH was studied. In Fig. S7C, with the increase of pH, the peak potential of AP has a negative migration, indicating that protons participate in the oxidation reaction [2]. The relationship between pH value and peak potential is $E(\mathrm{V}) = 0.6391 - 0.04857\ \mathrm{pH}$ ($R^2 = 0.9984$). The slope of Nernst equation is $\mathrm{E} = \mathrm{E}^\theta - (0.059\ \mathrm{m/n})\ \mathrm{pH}$ [3], which means that the number of protons (m) and electrons (n) in charge transfer is basically equal. Therefore, pH value of 6.0 is selected as the optimal pH value of the electrolyte [4].

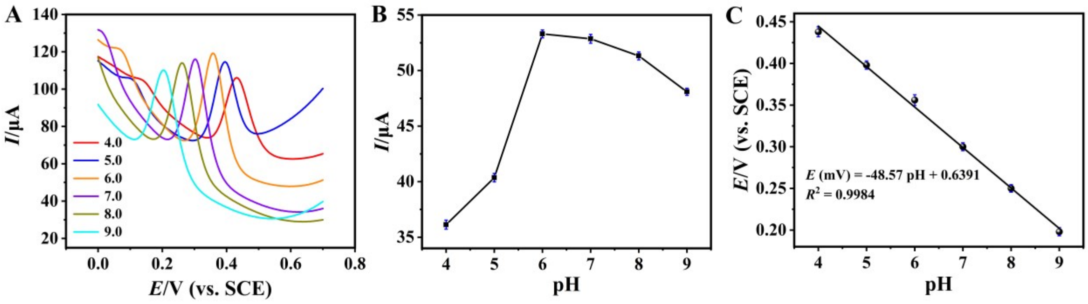

Fig. S7 SWV curves of 10 μM AP (A) at Mo_2C/GCE in 0.1 M PBS (pH 7.0) with different pH values (4.0, 5.0, 6.0, 7.0, 8.0, and 9.0). The effect of pH on peak current (B) and peak potential (C).

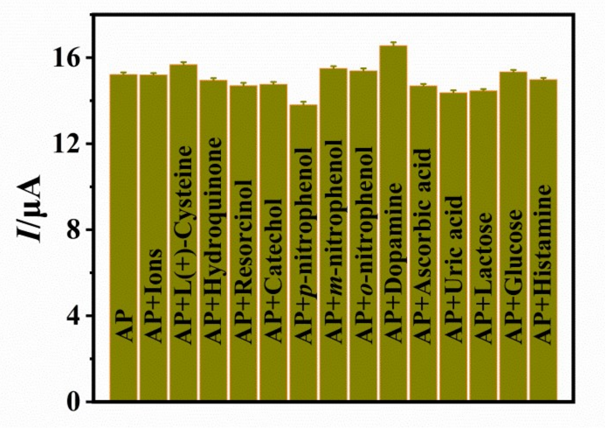

Fig. S8 (A) Sensing responses towards AP in the presence of decuple conentration of interfering substances using Mo_2C/GCE.

Table S1 Determination of AP in real samples by Mo_2C/GCE (n = 3)

Samples		Added (μM)	Found (μM)	Recovery (%)
Tap water	1	30	30.44	101.47
	2	50	49.76	99.52
River water	1	30	29.92	99.73
	2	50	50.51	101.02

Table S2 Determination of AP in real samples by UV-vis spectrometry (n = 3)

Samples		Added (μM)	Found (μM)	Recovery (%)
Tap water	1	30	29.74	99.13
	2	50	48.87	97.74
River water	1	30	31.63	105.43
	2	50	48.55	97.10

References

1. A. U. Alam, Y. Qin, M. M. Howlader, N.-X. Hu and M. J. Deen, *Sensors. Actuat B-Chem*, 2018, **254**, 896-909.
2. F. F. Lin, T. Wei, D. H. An, W. L. Wang and L. Z. Pei, *Surf. Eng. Appl. Electrochem*, 2018, **54**, 142-146.
3. Q. T. Hua, N. Ruecha, Y. Hiruta and D. Citterio, *Anal. Methods*, 2019, **11**.
4. Z. Jing, J. Ma, Y. Zhang, H. Lei and Q. Wan, *J. Chem. Technol. Biot*, 2014, **89**, 259-264.